Shock-Augmented Ignition Approach to Laser Inertial Fusion

R. H. H. Scott,[1,*] D. Barlow,[1] W. Trickey,[2] A. Ruocco,[1] K. Glize,[1] L. Antonelli,[2] M. Khan,[2] and N. C. Woolsey[2]
[1]Central Laser Facility, STFC Rutherford Appleton Laboratory, Harwell Oxford, OX11 0QX, United Kingdom
[2]York Plasma Institute, School of Physics, Engineering and Technology, University of York, York, YO10 5DD, United Kingdom

(Received 23 June 2021; revised 24 August 2022; accepted 21 September 2022; published 2 November 2022)

Shock ignition enables high gain at low implosion velocity, reducing ablative Rayleigh-Taylor instability growth, which can degrade conventional direct drive. With this method, driving a strong shock requires high laser power and intensity, resulting in inefficiencies in the drive and the generation of hot electrons that can preheat the fuel. A new "shock-augmented ignition" pulse shape is described that, by preconditioning the ablation plasma before launching a strong shock, enables the shock ignition of thermonuclear fuel, but importantly, with substantially reduced laser power and intensity requirements. The reduced intensity requirement with respect to shock ignition limits laser-plasma instabilities, such as stimulated Raman and Brillouin scatter, reducing the risk of hot-electron preheat and restoring the laser coupling advantages of conventional direct drive. Simulations indicate that, due to the reduced power requirements, high gain (~100) ignition of large-scale direct drive implosions (outer radius ~1750 μm, deuterium-tritium ice thickness ~165 μm) may be possible within the power and energy limits of existing facilities such as the National Ignition Facility. Moreover, this concept extends to indirect drive implosions, which exhibit substantial yield increases at reduced implosion velocity. Shock-augmented ignition expands the viable design space of laser inertial fusion.

DOI: 10.1103/PhysRevLett.129.195001

Laser inertial confinement fusion [1] uses a spherical implosion to integrate incident photon flux in space and time, converting it first into implosion kinetic energy, then, at stagnation, into internal energy. In direct drive, the lasers impinge directly on the implosion capsule. Indirect drive uses a high-Z enclosure (a hohlraum) to absorb the laser energy before it is reemitted as x rays, which drive the implosion. The capsule is a spherical low-Z shell containing deuterium (D) and tritium (T) fuel. The low-Z shell ablates; photon absorption raises the pressure of the shell's exterior, driving an outward plasma expansion that, through conservation of momentum, accelerates the shell inward. In this way, a significant fraction of the incident photon flux is absorbed, a proportion of which is converted into implosion kinetic energy. As the implosion proceeds, volume reduction due to spherical convergence, combined with shock heating, creates a low-density, hot, and high-pressure "hot spot" at the center of the dense fuel shell. This central pressure decelerates the converging shell, converting the shell's kinetic energy into internal energy, compressing the DT hot spot and shell. If the compressed hot spot's temperature (T) and density-radius product (ρR) are sufficient ($\rho R > 0.3$ g cm^{-2}, $T > 5$ keV), fusion α particles are emitted that stop within the hot spot, further heating it, causing additional α-particle emission. A thermonuclear burn wave then propagates into the surrounding dense fuel shell, creating net energy release: ignition.

Laser inertial-fusion implosion designs seek to optimally balance multiple implosion degradation mechanisms. The shock-augmented ignition (SAI) concept described in this Letter enables a strong shock to be generated without the requirement for high peak intensity or power in laser direct drive, nor the requirement for extreme radiation temperature rise rates in indirect drive. In doing so, it combines the advantages of shock ignition with those of central hot spot ignition [2]. This reduces challenges associated with the growth of the Rayleigh-Taylor instability (RTI) [3,4] caused by the high implosion velocity required for central hot spot ignition and those caused by laser-plasma instabilities [5] due to the high laser intensities required for shock ignition (SI) [6]. The key innovation of the SAI approach is the introduction of a brief reduction in laser power preceding a rapid rise in power. The dip in the flux driving the ablation process acts to precondition the ablation plasma in the shock-formation region; then once the laser power rises again, the characteristics of the preconditioned ablation plasma aid shock generation.

Direct drive central hot spot (DD_{CHS}) designs are restricted to laser intensities $\lesssim 1.3 \times 10^{15}$ W cm^{-2} to reduce the impact of laser-plasma instabilities (LPIs) [7]. Two plasmon decay [8] and stimulated Raman scatter (SRS) [9] stimulate the growth of electron-plasma waves (EPWs) in the underdense ablated plasma. The EPWs accelerate electrons to high energy; these "hot electrons" can then deposit energy within the imploding DT fuel, potentially preheating it, thereby reducing the fuel's compressibility [2]. Reflectivity caused by SRS and

stimulated Brillouin scatter (SBS) [10] reduces laser coupling, while crossed beam energy transfer can change the spatiotemporal distribution of laser light, further reducing laser-to-implosion energy coupling [11]. While exact LPI thresholds and growth rates depend on the particular instability, all LPIs exhibit strong laser intensity dependence prior to saturation (e.g., see Ref. [12] and references therein).

In principle, LPIs in direct drive could be kept below threshold by employing a large radius implosion shell; the increased surface area would reduce the required incident laser intensity. However, the increased shell radius increases the shell in-flight aspect ratio (IFAR = shell inner radius/shell thickness) for a given shell mass. Higher IFAR implosions are more susceptible to RTI, as RTI "fingers" of higher Z ablator material can penetrate the thin in-flight fuel shell, degrading performance, principally by enhancing hot spot radiative emissions. IFAR can be reduced by reducing the shell compressibility, which is inversely proportional to the adiabat α, where $\alpha = P_{\mathrm{sh}}/P_{\mathrm{Fermi}}$, P_{sh} is the cold fuel shell's pressure, and P_{Fermi} is the Fermi degenerate pressure. α is mainly set by the strength of the early-time shocks in inertial confinement fusion implosions. While increasing α improves IFAR and hence robustness to RTI, the reduction in compressibility, and hence convergence, reduces the maximum obtainable implosion performance (i.e., that from 1D simulations).

Implosion designs therefore trade off these characteristics in an attempt to balance 1D performance against RTI, preheat, and laser coupling concerns. If the implosion mass can be increased, this ameliorates numerous difficulties: the shell is thicker for a given initial radius, reducing IFAR and hence susceptibility to both RTI and preheat. For a laser energy E_L to implosion kinetic energy E_k, the coupling efficiency is $\eta = E_k/E_L$. For a given implosion velocity v_{sh}, the shell mass then scales as $m_{\mathrm{sh}} \sim 2E_L\eta/v_{\mathrm{sh}}^2$. So it can be increased by (1) increasing incident laser energy, (2) increasing laser-to-implosion kinetic-energy coupling efficiency, or (3) by reducing implosion velocity. In comparison to indirect drive, $\mathrm{DD_{CHS}}$ couples 5–6 times more laser energy to implosion kinetic energy [13], but is more subject to RTI growth due to "seeds" created by localized laser intensity inhomogeneities (speckles) and reduced RTI stabilization due to the shorter ablation-front density scale lengths and smaller mass-ablation rates [14].

Shock ignition [15] is a variant of laser direct drive that has the potential for high fusion energy gain (≥ 200 [16,17]) combined with increased robustness to RTI. Rather than relying purely on the conversion of kinetic energy to internal energy, as per central hot spot ignition, SI uses a rapid rise in laser power toward the end of the pulse shape to launch a strong shock into the preassembled fuel. The additional shock heating and compression reduces the implosion velocity required for ignition. This reduces susceptibility to RTI as less acceleration is required, while, for a given laser energy, more fuel mass can be imploded, improving both IFAR and yield.

The hydrodynamic advantages of SI are clear, however, its requirement for high laser intensity, and hence power [18], creates challenges; launching a sufficiently strong shock requires peak intensities of $\sim 10^{16}$ W cm^{-2}—well above LPI thresholds, meaning SI is susceptible to low laser coupling and preheat. Although due to the increased shell areal density at the time of the laser power spike, sufficiently low hot-electron temperatures may enhance shock generation [19]. The intensity requirement also places limitations on the implosion-capsule diameter which can be fielded on existing facilities. For example, assuming the National Ignition Facility's (NIF's) peak power of 520 TW and spherical illumination at 1×10^{16} W cm^{-2} limits the capsule diameter to 1260 μm and hence the implosion energy scale. SI designs [20] that use a combination of small and large focal spots to increase the implosion energy scale to 750 kJ and radius 1030 μm are promising, but remain below NIF's full energy.

By launching a strong shock using moderate power and intensity, the SAI concept combines the advantages of $\mathrm{DD_{CHS}}$ with those of SI. By operating at moderate laser intensity, $\mathrm{DD_{CHS}}$ achieves high laser absorption and limits the impact of LPIs and hot electrons. Additionally, the moderate peak power requirements of $\mathrm{DD_{CHS}}$ mean large diameter implosion capsules can be fielded, reducing the hot spot pressure requirement for ignition [14] and sensitivity to fixed-scale RTI seeds. Furthermore, the SI (and SAI) approach improves robustness to the Rayleigh-Taylor instability by reducing the implosion velocity and increasing fuel mass.

In order to evaluate the SAI concept, one-dimensional simulations have been performed with the Hyades [21] Lagrangian radiation-hydrodynamics code. This employs laser energy deposition via inverse bremsstrahlung, flux-limited thermal conductivity (electron flux limiter = 0.06), (70 group) diffusive multigroup radiation and multigroup thermonuclear burn-product transport–energy deposition, and first-principles equation of state [22] equations of state.

An example 1.9 MJ direct drive SAI pulse shape and implosion-capsule design using 351 nm laser wavelength is shown in Fig. 1. Both $\mathrm{DD_{CHS}}$ (black) and SAI (red) pulse shapes employ a low-adiabat laser pulse shape, with a shell mass averaged $\alpha \sim 1.2$, a 165 μm thick DT-ice layer, 51 μm wall CH ablator and 1751 μm outer radius. The SAI ($\mathrm{DD_{CHS}}$) designs have peak powers and intensities of 510 (365) TW and 1.3×10^{15} (0.93×10^{15}) W cm^{-2}, respectively. The $\mathrm{DD_{CHS}}$ implosion marginally fails to ignite with a yield of 900 kJ while the SAI implosion ignites with a gain of $\sim$100 (190 MJ yield). The SAI implosion velocity is 315 km/s: 10% lower than the 345 km/s of the $\mathrm{DD_{CHS}}$ implosion. Simulations with α-particle deposition turned off reveal that the SAI ($\mathrm{DD_{CHS}}$) peak pressure is 1400 (310) Gbar.

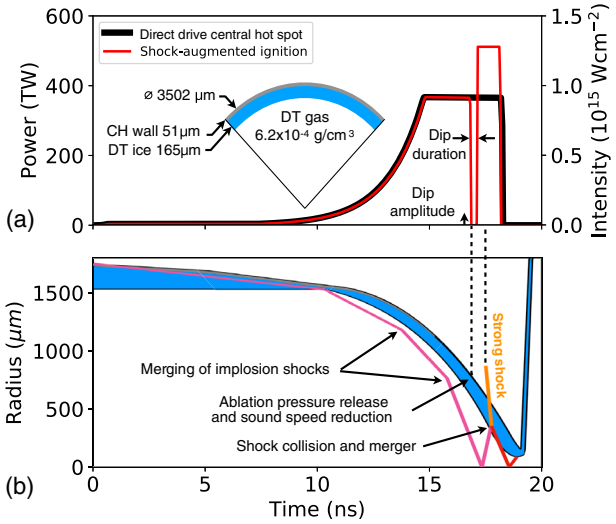

FIG. 1. (a) 1.9 MJ direct drive laser pulse shapes: a central hot spot design (black) and SAI pulse shape (red). Note in this extreme case, dip amplitude is 0 TW. Inset: 1.9 MJ implosion-capsule design. (b) Schematic showing key implosion features: the blue region is the DT ice. The magenta line depicts the trajectory of the innermost shock that results from the launching and subsequent merging of the "conventional" shocks created by the pulse shape. The trajectory of the SAI shock is shown in orange. It collides with the rebound shock near the DT-ice inner surface; the resulting merged shock is shown in red. The dip in power preconditions the ablation plasma, aiding shock generation. This enables a strong shock to be launched without the requirement for very high power or intensity. Vertical dashed black lines are to guide the reader's eye.

Importantly, if the power dip is retained, but the spike power is reduced to that of the flattop (365 TW), the shock strength is reduced, but a shock is still generated. The addition of the power dip alone enables the recovery of ignition with gain ~90.

Retaining the above capsule and early-time pulse shape and instead using a SI power spike (and no power dip), we find a peak intensity of 1×10^{16} W cm^{-2} is required to create the same ~4 Gbar shock strength as the above 510 TW SAI design. It ignites with the same gain; however, at 4000 TW, the peak power greatly exceeds that available on existing facilities. Previous simulations [16,23] have shown that at this energy scale (1.9 MJ) SI does not require such high intensity to drive the shock, although these evaluations did not include LPI energy losses. To investigate this, peak powers of 2000, 1000, and 510 TW were evaluated. It was found that, by varying the spike timing, a gain of 100 was recovered. Importantly, however, at these powers no igniter shock forms. Instead, it is found that these targets are accelerated to higher velocity (~355 km/s), recovering ignition. While these targets do ignite, this regime is, to our best evaluations, an example of conventionally ignited implosions; the increase in implosion velocity raises it above the self-ignition velocity threshold, causing ignition. An initial evaluation of the relative SRS and SBS levels in CHS, SAI, and SI is shown in the Supplemental Material [24], which includes Refs. [25–28].

A hydrodynamic shock forms when a fluid-pressure increase induces ion-acoustic wave speeds exceeding the local sound speed; the ion-acoustic waves are unable to propagate faster than the local sound speed, so the ion-acoustic wave amplitudes combine locally, creating a pressure discontinuity, or shock. Such conditions are induced by a rapid increase in pressure, specifically a strong positive temporal derivative of pressure $\delta P/\delta t$, where $\delta P = P_1 - P_0$ and $\delta t = t_1 - t_0$ and subscripts 0 and 1 refer to the initial and final states, respectively. For shocks driven by laser ablation, the required pressure change is induced by a change in laser intensity [$P_{\mathrm{abl}} \propto (I_L/\lambda_L)^{2/3}$] [29], where I_L and λ_L are the laser intensity and wavelength, respectively. The magnitude of $\delta P/\delta t \propto (I_1 - I_0)/\delta t$. δt is the duration of the rise to peak power, which is dictated by laser-system limitations; here we assume δt is minimized, to maximize $\delta P/\delta t$.

In SI, the power spike causes a rapid intensity rise that induces a pressure increase, creating a shock. In this scenario, I_0 is the intensity "flattop" before the power spike (e.g., $t = 15$ ns in Fig. 1) and I_1 the spike intensity. If one wanted to reduce the peak intensity I_1 (to ameliorate LPIs, for example) but maintain δP, it is only possible to do so by also reducing I_0. However, for a given shell mass, the amplitude and duration of I_0 largely dictate the implosion velocity, so excessive reduction of I_0 would preclude ignition; the shock only *supplements* the internal energy provided by the implosion's kinetic energy, and so can only compensate for a finite reduction in velocity.

The SAI pulse shape circumvents this limitation by introducing a brief reduction in power before the power spike. This power dip preconditions the ablation plasma, aiding shock generation in two ways. The reduced laser intensity reduces the ablation-plasma electron temperature which, through electron-ion equilibration, lowers both the local sound speed [30] [see Figs. 2(a) and 2(b)] and pressure. This reduction in sound speed means the ion wave speed required to form a shock reduces, which in turn reduces the $\delta P/\delta t$ required for shock formation. Furthermore, as the initial plasma pressure (P_0) in the shock-formation region is reduced, when the laser intensity is increased, a larger $\delta P/\delta t$ is possible for a given maximum intensity, further aiding shock formation.

Simulations indicate that the SAI laser pulse shape forms a strong shock, even though the peak intensity is restricted to 1.3×10^{15} W cm^{-2}. The energy invested in shock formation is ~1/4 of the total laser energy. Once formed, spherical convergence amplifies the SAI shock pressure by a factor of ~100 as it propagates inward, as per SI. Depending on the details of the pulse shape, this shock is 2.5–7.5 Gbar in strength at the point where it merges with

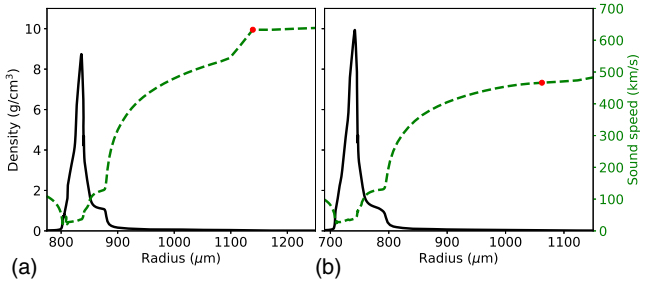

FIG. 2. SAI shell-density profiles (solid black line, left axes) and sound speeds (dashed green line, right axes): (a) just before the power dip and (b) at the end of the power dip. The sound speed at the critical surface (red dot) has decreased by 150 km/s during the power dip, while despite the laser being turned off, the fuel shell has actually increased in density slightly due to spherical convergence.

the return shock near the DT-ice inner surface, as shown in Fig. 3(b). This is equivalent strength to those of SI designs [e.g., see Fig. 3(a) in [15] or Fig. 6 in [31]].

Once the shock is formed via the SAI pulse shape, the hydrodynamics of hot spot formation and compression are the same as those of SI. However, the requirement for a power dip in the SAI laser pulse shape has the potential to compromise implosion performance by decompressing the DT fuel shell. This could deleteriously affect the implosion performance in two ways. First, if the DT fuel shell density is reduced at peak velocity, the final fully converged density, and hence shell ρR, are both reduced, limiting yield [29]. Secondly, the entropy added by a shock is $\delta S \propto \delta P/\rho^{5/3}$, where δP is the pressure change across the shock and ρ is the density of the material ahead of the shock. Consequently, if the fuel shell density is too low, the shock will add excessive entropy, reducing the DT-shell compressibility, again limiting shell ρR.

Simulations indicate it is possible to control fuel shell decompression. Figure 3(a) shows that the preshock fuel shell density at peak velocity (well after the power dip) is very similar using both SAI and DD_{CHS} pulse shapes. However, the potential for shell decompression places limitations on the SAI power dip duration and amplitude [see Fig. 1(a)]. Longer-duration, lower-power dips maximize shock strength, but if the duration is excessive and the power too low, the shell decompresses, meaning optimized SAI designs must balance shell decompression against shock strength.

Shell decompression can be countered by either restricting the power dip duration or by using a nonzero amplitude. As the power dip amplitude is increased (the dip is less deep), the optimal duration for strong shock generation increases. Figure 4(a) depicts a set of optimized 1.9 MJ direct drive SAI pulse shapes. For a given power dip amplitude, the dip duration and timing have been approximately optimized. For each optimized pulse shape shown, the strength of the shock is approximately equal.

Figure 4(b) depicts the corresponding yield curves as a function of shock delay for the various dip amplitudes; the timing window is ≥ 0.5 ns—within the capabilities of existing laser facilities. Interestingly, the variant with a higher-amplitude, longer-duration power dip has marginally higher yields and a wider timing window. This result is encouraging, as such laser pulse shapes are likely to be easier for laser facilities to accommodate.

Hydrodynamic scaling [32] of the laser pulse and target shown in Fig. 1 indicates that ignition via SAI may be possible with ~350 kJ of laser energy, although energy gain was reduced to ~35 at this scale. At 28 kJ, as per Omega [33], SAI increased hot spot pressure by 30% to 100 Gbar.

Previous work on indirect drive SI [34] found that a 200–300 eV radiation temperature rise in ~1 ns is required to launch a 300 Mbar shock; a stringent requirement given 3 ns is typically required [35]. Indirect drive SAI viability was evaluated using Hyades simulations of x-ray driven implosions. The design basis was NIF shot N210808. Using the as-shot radiation temperature vs time and capsule

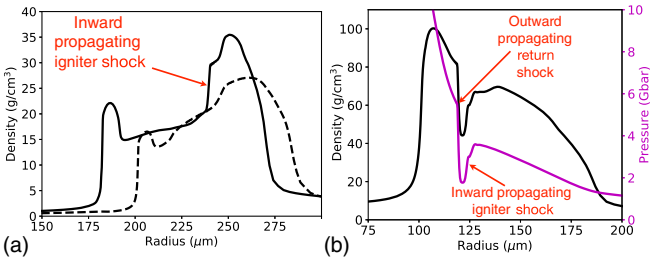

FIG. 3. (a) Density profiles at peak velocity (~200 ps after the laser pulse ended): solid (dashed) lines show the profile with (without) the SAI dip then rise in power, illustrating control of shell decompression. (b) SAI density and pressure (right axis) profiles just prior to the merger of the return shock and the igniter shock, near the DT-ice inner surface. The shock pressure is ~4 Gbar.

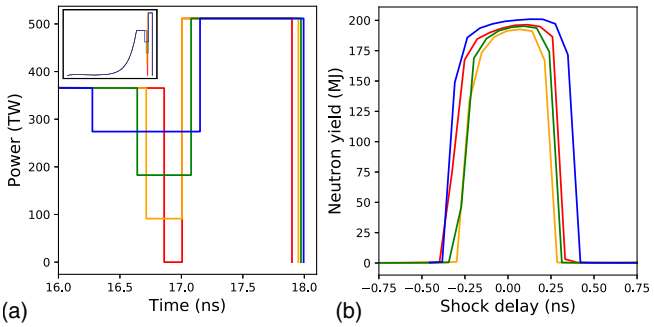

FIG. 4. (a) Laser power dip and spike details of the optimally timed 1.9 MJ laser pulse shapes. Inset: the whole laser pulse shape; up to 16 ns it is the same as that shown in Fig. 1. (b) Thermonuclear energy yield as a function of the timing of the power dip and spike, and hence shock, for 1.9 MJ implosions.

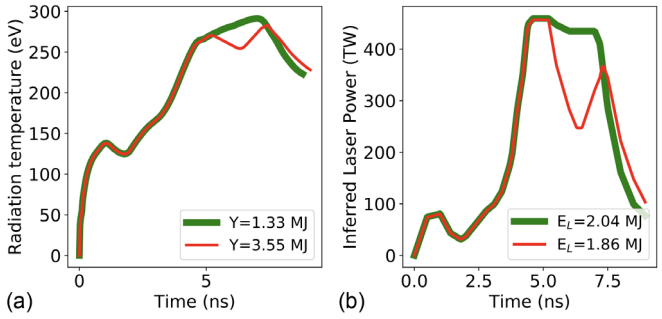

FIG. 5. (a) Indirect drive pulse shapes used to evaluate the SAI concept: an example three-shock N210808-like central hot spot implosion that yields 1.33 MJ (green), while a SAI pulse shape yields 3.55 MJ at reduced velocity (red). Integrated incident x-ray flux is the same in both cases. (b) Inferred laser power and energy (E_L) required for (a) using an analytical hohlraum model [34].

dimensions [36], simulations were tuned to match experimental observables with an implosion velocity of 400 km/s, yield of 1.33 MJ, and mass-averaged adiabat at maximum velocity ~3.5. A dip in radiation temperature during peak power was then applied, as shown in Fig. 5. The yield increased to 3.55 MJ, while the implosion velocity decreased by 80 km/s to 322 km/s. Additionally, the stability of the ice-ablator interface approaching and at maximum velocity is substantially improved. Thus, SAI has the potential to enhance thermonuclear yield while reducing susceptibility to the RT instability. This may enable future designs to operate at lower adiabats, further enhancing yield. We highlight that the rise rate required for SAI (40 eV/ns) is less than half that required for indirect drive SI and lower than the maximum rise rate of N210808, increasing the feasibility of fielding such experiments on the NIF.

In summary, we have described a novel laser direct drive pulse-shaping concept that, by introducing a brief reduction in laser power, enables the generation of a strong shock (~4 Gbar) while keeping the laser intensity below 1.3×10^{15} W cm^{-2}. As per shock ignition, this shock collides with the return shock near the DT-ice inner surface, heats the hot spot ions, and aids fuel compression. This enables the ignition of more fuel mass at lower implosion velocity, increasing thermonuclear yield and RTI robustness, for a given laser energy. In comparison to shock ignition, SAI's reduced intensity requirements should significantly reduce laser-plasma instabilities, increasing laser coupling and reducing hot-electron preheat. Furthermore, due to the reduced power requirement, it may be possible to shock ignite large-scale direct drive implosions using SAI within the power and energy limits of existing laser facilities such as NIF. These larger diameter implosion capsules have reduced hot spot pressure requirements for ignition, and due to SAI's reduced velocity requirement, are predicted to be less susceptible to RTI than equivalent-scale DD_{CHS} designs. An initial evaluation of the applicability of SAI to indirect drive shows that, at fixed laser energy and substantially reduced implosion velocity, an increase in yield is predicted.

Shock-augmented ignition has the potential to expand the viable ignition design space of laser inertial fusion and move experiments toward fusion energy gain.

This work was funded by EPSRC Grants No. EP/P023460/1 and No. EP/P026796/1. R. H. H. S. would like to thank D. Callahan, O. Hurricane, A. Kritcher, O. Landen, K. Newman, R. Nora, H. Robey, V. Smalyuk, C. Weber, A. Zylstra, and others at Lawrence Livermore National Laboratory for their various ongoing contributions.

Note added.—Recently, extensive discussions regarding indirect drive experiments to evaluate this concept on NIF have taken place.

*Robbie.Scott@stfc.ac.uk

[1] J. Nuckolls, L. Wood, A. Thiessen, and G. Zimmerman, Nature (London) **239**, 139 (1972).
[2] D. Barlow, T. Goffrey, K. Bennett, R. H. H. Scott, K. Glize, W. Theobald, K. Anderson, A. A. Solodov, M. J. Rosenberg, M. Hohenberger, N. C. Woolsey, P. Bradford, M. Khan, and T. D. Arber, Phys. Plasmas **29**, 082704 (2022).
[3] L. Rayleigh, *Scientific Papers* (Cambridge University Press, Cambridge, England, 1900).
[4] G. I. Taylor, Proc. R. Soc. A **201**, 192 (1950).
[5] W. L. Kruer, *The Physics of Laser Plasma Interactions* (Addison-Wesley, Reading, MA, 1988), Vol. 45, p. 135.
[6] R. H. H. Scott, K. Glize, L. Antonelli, M. Khan, W. Theobald, M. Wei, R. Betti, C. Stoeckl, A. G. Seaton, T. D. Arber, D. Barlow, T. Goffrey, K. Bennett, W. Garbett, S. Atzeni, A. Casner, D. Batani, C. Li, and N. Woolsey, Phys. Rev. Lett. **127**, 065001 (2021).
[7] M. J. Rosenberg, A. A. Solodov, J. F. Myatt, W. Seka, P. Michel, M. Hohenberger, R. W. Short, R. Epstein, S. P. Regan, E. M. Campbell, T. Chapman, C. Goyon, J. E. Ralph, M. A. Barrios, J. D. Moody, and J. W. Bates, Phys. Rev. Lett. **120**, 055001 (2018).
[8] A. Simon, R. W. Short, E. A. Williams, and T. Dewandre, Phys. Fluids **26**, 3107 (1983).
[9] M. N. Rosenbluth, Phys. Rev. Lett. **29**, 565 (1972).
[10] C. L. Tang, J. Appl. Phys. **37**, 2945 (1966).
[11] I. V. Igumenshchev, D. H. Edgell, V. N. Goncharov, J. A. Delettrez, A. V. Maximov, J. F. Myatt, W. Seka, A. Shvydky, S. Skupsky, and C. Stoeckl, Phys. Plasmas **17**, 122708 (2010).
[12] D. S. Montgomery, Phys. Plasmas **23**, 055601 (2016).
[13] R. Betti and O. A. Hurricane, Nat. Phys. **12**, 435 (2016).
[14] R. S. Craxton *et al.*, Phys. Plasmas **22**, 110501 (2015).
[15] R. Betti, C. D. Zhou, K. S. Anderson, J. L. Perkins, W. Theobald, and A. A. Solodov, Phys. Rev. Lett. **98**, 155001 (2007).
[16] A. J. Schmitt, J. W. Bates, S. P. Obenschain, S. T. Zalesak, and D. E. Fyfe, Phys. Plasmas **17**, 042701 (2010).
[17] S. Atzeni, A. Marocchino, A. Schiavi, and G. Schurtz, New J. Phys. **15**, 045004 (2013).

[18] D. Batani, S. Baton, A. Casner, S. Depierreux, M. Hohenberger, O. Klimo, M. Koenig, C. Labaune, X. Ribeyre, C. Rousseaux, G. Schurtz, W. Theobald, and V. Tikhonchuk, Nucl. Fusion **54**, 054009 (2014).
[19] A. R. Bell and M. Tzoufras, Plasma Phys. Controlled Fusion **53**, 045010 (2011).
[20] K. S. Anderson, R. Betti, P. W. McKenty, T. J. B. Collins, M. Hohenberger, W. Theobald, R. S. Craxton, J. A. Delettrez, M. Lafon, J. A. Marozas, R. Nora, S. Skupsky, and A. Shvydky, Phys. Plasmas **20**, 056312 (2013).
[21] J. T. Larsen and S. M. Lane, J. Quant. Spectrosc. Radiat. Transfer **51**, 179 (1994), Special Issue Radiative Properties of Hot Dense Matter.
[22] S. X. Hu, B. Militzer, V. N. Goncharov, and S. Skupsky, Phys. Rev. B **84**, 224109 (2011).
[23] S. Atzeni and G. Schurtz, in Diode-Pumped High Energy and High Power Lasers; ELI: Ultrarelativistic Laser-Matter Interactions and Petawatt Photonics; and HiPER: The European Pathway to Laser Energy, edited by L. O. Silva, G. Korn, L. A. Gizzi, C. Edwards, and J. Hein, International Society for Optics and Photonics (SPIE, Bellingham, WA, 2011), Vol. 8080, pp. 302–313.
[24] See Supplemental Material at http://link.aps.org/supplemental/10.1103/PhysRevLett.129.195001 contains an initial evaluation of the anticipated effects of stimulated Raman and Brillouin scatter laser plasma instabilities in the three direct drive scenarios examined in this paper: Shock Ignition, Shock Augmented Ignition, and Central Hotspot.
[25] A. Nutter, R. Scott, and N. Woolsey (to be published).
[26] L. Hao, R. Yan, J. Li, W. D. Liu, and C. Ren, Phys. Plasmas **24**, 062709 (2017).
[27] S. P. Regan *et al.*, Phys. Rev. Lett. **117**, 025001 (2016).
[28] V. Gopalaswamy *et al.*, Nature (London) **565**, 581 (2019).
[29] S. Atzeni and J. Meyer-ter Vehn, *The Physics of Inertial Fusion* (Oxford University Press, Oxford, 2004).
[30] J. Huba, Nrl plasma formulary (2007), https://search.library.wisc.edu/catalog/9999968650002121/cite.
[31] S. Atzeni, X. Ribeyre, G. Schurtz, A. Schmitt, B. Canaud, R. Betti, and L. Perkins, Nucl. Fusion **54**, 054008 (2014).
[32] R. Nora, R. Betti, K. S. Anderson, A. Shvydky, A. Bose, K. M. Woo, A. R. Christopherson, J. A. Marozas, T. J. B. Collins, P. B. Radha, S. X. Hu, R. Epstein, F. J. Marshall, R. L. McCrory, T. C. Sangster, and D. D. Meyerhofer, Phys. Plasmas **21**, 056316 (2014).
[33] T. Boehly, D. Brown, R. Craxton, R. Keck, J. Knauer, J. Kelly, T. Kessler, S. Kumpan, S. Loucks, S. Letzring, F. Marshall, R. McCrory, S. Morse, W. Seka, J. Soures, and C. Verdon, Opt. Commun. **133**, 495 (1997).
[34] W. Trickey and J. Pasley, Plasma Phys. Controlled Fusion **61**, 105010 (2019).
[35] T. R. Dittrich, O. A. Hurricane, D. A. Callahan, E. L. Dewald, T. Doppner, D. E. Hinkel, L. F. Berzak Hopkins, S. Le Pape, T. Ma, J. L. Milovich, J. C. Moreno, P. K. Patel, H.-S. Park, B. A. Remington, J. D. Salmonson, and J. L. Kline, Phys. Rev. Lett. **112**, 055002 (2014).
[36] A. B. Zylstra, A. L. Kritcher, O. A. Hurricane, D. A. Callahan, J. E. Ralph, D. T. Casey, A. Pak, O. L. Landen, B. Bachmann, K. L. Baker *et al.* Phys. Rev. E **106**, 025202 (2022).